

Analysis of Biomass Co-Firing Impact on Boiler Tube Corrosion Rate in Steam Power Plants

¹*Rifqi Jauhari, ²Hadiyanto, ³Sri Widodo Agung Suedy

^{1,2,3}Master Program in Energy, Graduate School, University of Diponegoro, Semarang, Indonesia

*Corresponding Author's E-mail: rifqijauhari@students.undip.ac.id

Abstract - Biomass co-firing in coal-fired power plants is a key strategy to support national renewable energy targets. Although technically feasible, its implementation may affect boiler reliability and plant performance. This study evaluates the impact of co-firing on corrosion rate, boiler tube remaining life, Net Plant Heat Rate (NPHR), and Specific Fuel Consumption (SFC) using Two-Way ANOVA and linear regression. Results show that area/location, fuel type, and their interaction significantly affect corrosion rate and remaining life ($p < 0.05$). Fuel type is the dominant factor, with partial eta squared (η^2_p) values 0.900 (Unit 1), 0.812 (Unit 2) in corrosion rate and 0.915 (Unit 1) and 0.901 (Unit 2) in remaining life. Regression analysis indicates that calorific value influences NPHR and SFC, with both positive and negative relationships depending on unit and fuel composition. Overall, the implementation of biomass co-firing has a significant impact on corrosion rate, remaining life, and changes in power plant performance. Nevertheless, co-firing remains a viable energy transition solution, provided that technical considerations and appropriate operational control strategies are properly addressed.

Keywords: Co-Firing, Corrosion Rate, Remaining Life, NPHR, SFC.

I. INTRODUCTION

Co-firing has been established as one of the strategic initiatives under PLN's green booster program. PLN is spearheading the program with the grand ambition of using biomass cofiring across its 144 CFPPs, a goal which essentially requires the creation of a large-scale biomass industry across the Country [1]. The Indonesian state-owned electricity company aims to accelerate the achievement of a 23% renewable energy mix target by 2025 through the utilization of existing power plant infrastructure and waste management solutions. The total capacity of PLN's coal-fired power plants (CFPPs) with co-firing capability reaches 18.9 GW. If CFPPs implement co-firing at ratios of 6% for Pulverized Coal (PC) boilers, 40% for Circulating Fluidized Bed (CFB) boilers, and 70% for stoker boilers, this would be equivalent to an additional renewable energy capacity of

approximately 2.7 GW per year (assuming a 70% capacity factor) [2],[3].

Co-firing activities have been implemented across several PLN power plant locations since 2020, covering various boiler types, including PC, CFB, and stoker systems. The biomass types utilized include urban solid waste [4] sawdust, palm kernel shells [5], pistachio shells [6] wood chips, wood pellets [7],[8], rice husk [9],[10], coconut shells, empty fruit bunches (EFB), Solid Recovered Fuel (SRF) pellets [11], water hyacinth, and corn cobs [3],[12].

Cofiring biomass with coal in power plants provides several advantages, including increased thermal efficiency, lower sulphur emissions, reduced costs and no need for continuous biomass supply because power plants can still use coal if biomass is not available [13]. Biomass fuel in the form of sawdust is blended with coal in the coal storage system to achieve a homogeneous mixture. The blended fuel is then conveyed through the coal feeder to the coal bunker and subsequently fed into the pulverizing mill. Prior to entering the boiler, the fuel mixture undergoes a grinding process in the pulverized mill to achieve a fineness of approximately 200 mesh, with more than 70% passing this size. Fineness sampling is typically conducted at the mill outlet pipe [14], mixtures of coal and biomass burning energy variability are influenced by carbon ash content, and biomass mixing will help to efficiently burn coal with low ash content [15].

Overall, a total of 114 coal-fired power plant units operated by PLN have the potential to implement biomass cofiring. These plants are distributed across 52 locations, with a combined installed capacity of approximately 18.1 GW, and are estimated to require around 9 million tons of biomass annually. The boiler technologies employed include 45 Pulverized Coal (PC) units with a total capacity of 15.5 GW, 39 Circulating Fluidized Bed (CFB) units with a capacity of 2.4 GW, and the remaining 30 units utilizing stoker boilers. The maximum co-firing ratios are approximately 5% for both PC and CFB boilers, while stoker boilers can accommodate up to 30% biomass blending [16].

Based on the data presented, further analysis is required to comprehensively evaluate the implementation of biomass

co-firing in Unit 1 and Unit 2 of PLTU Banten 2 Labuan. This study is intended to evaluate and compare the corrosion behavior of boiler tubes under conventional coal combustion and biomass co-firing conditions, with the objective of identifying significant variations in material degradation resulting from changes in fuel composition and combustion characteristics [17]. In addition, the analysis seeks to examine variations in the remaining life of boiler tubes when operating under co-firing conditions, providing insight into the long-term reliability and maintenance implications. Furthermore, the study investigates the influence of calorific value and the proportion of co-firing utilization on the Net Plant Heat Rate (NPHR), as a key indicator of thermal efficiency. Lastly, the effect of calorific value and co-firing operation on Specific Fuel Consumption (SFC) is evaluated to determine overall fuel efficiency performance and operational effectiveness of the plant under biomass integration.

II. MATERIAL AND METHODS

This study adopts a quantitative design to systematically investigate both material degradation and operational performance at PLTU Banten 2 Labuan. The quantitative approach is applied to evaluate the boiler tube thinning rate and overall power plant performance under varying fuel conditions. Furthermore, a structured approach is undertaken to identify and quantify the expected impacts of biomass co-firing on boiler tube integrity, particularly in relation to corrosion and remaining life. In parallel, the study examines the influence of biomass utilization on key performance indicators of the power plant, thereby providing an integrated assessment of both reliability and efficiency implications associated with co-firing implementation.

2.1 Operational and Performance Data

The data acquisition strategy employed in this study was designed to ensure high accuracy, consistency, and representativeness of operational conditions. Primary data related to fuel utilization, including coal and biomass consumption, were obtained from the plant's operational monthly report. These records provide time-resolved information on total electricity production, fuel (coal and biomass) consumption, and calorific value both of fuel, enabling a detailed characterization of co-firing practices under real plant conditions. To enhance data reliability, cross-validation was conducted using daily operation reports and fuel handling system records.

Operational performance parameters, including Net Plant Heat Rate (NPHR) and Specific Fuel Consumption (SFC), were derived from validated plant performance calculations based on real-time operating data. NPHR was calculated by correlating total fuel energy input with net electrical output,

while SFC was determined by quantifying the mass of fuel required per unit of electricity generated. These parameters were computed over consistent time intervals to minimize transient effects and ensure comparability between coal-only and co-firing conditions. Data filtering and normalization techniques were applied to exclude outliers and non-steady-state operating conditions. Operational and maintenance data were collected from Unit 1 and Unit 2 of PLTU Banten 2 Labuan, including: tube thickness measurements on Primary/Cold Superheat (A10 Elbow, C9 Elbow, C9 Straight and F10 Elbow) as shown in Figure 1, Fuel composition coal and co-firing, Calorific values, NPHR and SFC.

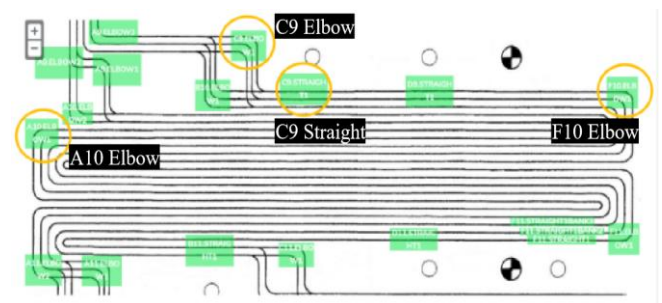


Figure 1: Boiler Mapping Primary/Cold Superheat

2.2 Coal and Biomass Blending Systems

Biomass co-firing is a combustion strategy that utilizes a specific blending ratio between coal and biomass-based fuels. The application of biomass co-firing technology in Coal-Fired Power Plants has been widely implemented across various countries and is increasingly recognized as a key transitional solution for reducing dependence on fossil fuels. This is largely attributed to its relatively straightforward integration into existing systems without requiring substantial modifications [18].

The deployment of biomass co-firing in the power generation sector is considered both economically viable and environmentally advantageous, making it an attractive alternative for sustainable energy transition. From an economic perspective, co-firing is regarded as cost-efficient due to its minimal capital investment requirements [19], as it leverages existing CFPP infrastructure and installed equipment. At the same time, it contributes to emission reduction and improved environmental performance compared to conventional coal combustion [20].

In PLTU Banten 2 Labuan use direct co-firing configurations, biomass is introduced as a secondary fuel alongside coal, which remains the primary fuel in the boiler system [21]. This approach offers several technical pathways, with four principal configurations commonly identified. The first option involves blending biomass directly with coal prior to injection into the existing combustion chamber. This

configuration is the simplest and most cost-effective in terms of implementation [22]. However, it presents notable operational risks, particularly related to boiler performance and material integrity. The presence of alkali compounds and other corrosive elements in biomass can promote deposition and fouling on heat transfer surfaces, potentially reducing boiler efficiency [18]. Moreover, the inherent differences in physical and chemical properties between coal and biomass may adversely affect combustion stability and flame characteristics. Consequently, this first approach is generally limited by the type of biomass that can be utilized, as well as by relatively low allowable co-firing ratios to maintain safe and stable boiler operation [23]. The direct co-firing operations in pulverized mill shown in the Figure 2.

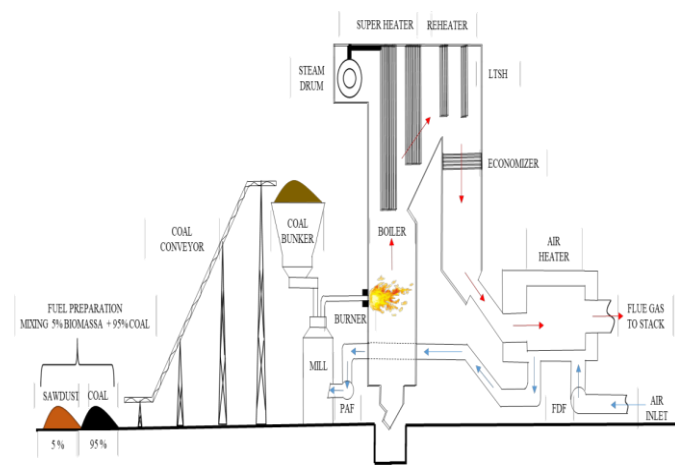


Figure 2: Direct Co-Firing in Pulverized Mill

2.3 Corrosion rate

The corrosion rate associated with thinning damage mechanisms is determined by calculating the difference between two thickness measurements divided by the time interval between those measurements. In practice, corrosion rate evaluation may incorporate thickness data collected at more than two inspection periods to improve accuracy and trend interpretation. Short-term corrosion rate is typically derived from the two most recent thickness measurements, providing a representation of current degradation behavior under prevailing operating conditions. In contrast, long-term corrosion rate is calculated using the latest thickness measurement in comparison with an earlier baseline measurement, usually taken at the beginning of the equipment’s service life. The comparison between short-term and long-term corrosion rates is particularly valuable, as discrepancies between these values can indicate changes in corrosion mechanisms or operating environments over time. The determination of both long-term and short-term corrosion rates can be carried in Eq. (1) and Eq. (2) [24]:

For long-term analysis:

$$Corrosion\ Rate\ (CR) = \frac{t_{initial} - t_{actual}}{\text{time between } t_{initial} \text{ and } t_{actual}} \quad (1)$$

For short-term analysis:

$$Corrosion\ Rate\ (CR) = \frac{t_{previous} - t_{actual}}{\text{time between } t_{previous} \text{ and } t_{actual}} \quad (2)$$

2.4 Remaining Life

Boiler tube remaining life refers to the estimated operational period during which a boiler tube can continue to function safely and reliably before reaching its minimum allowable thickness or failure limit [25]. The assessment of remaining life is an essential aspect of integrity management in Coal-Fired Power Plants, as boiler tubes are continuously exposed to high temperatures, pressure, corrosion, erosion, and cyclic thermal stresses during operation. The remaining life is generally determined by evaluating the current tube thickness, the original or design thickness, the minimum allowable thickness, and the measured corrosion or thinning rate. As material degradation progresses over time, the wall thickness of the tube gradually decreases, reducing its ability to withstand operational stresses. Therefore, periodic inspection and thickness monitoring are required to accurately predict the safe operating lifespan of the component. The remaining life of boiler tubes can be calculated using the following Eq. (3) [24]:

$$Remaining\ Life\ (RL) = \frac{t_{actual} - t_{required}}{\text{corrosion rate}} \quad (3)$$

2.5 NPHR and SFC

Heat rate represents the amount of thermal energy required to generate a specific quantity of electrical energy (kWh). A lower heat rate indicates better machine or power plant performance, as less thermal energy is needed to produce electricity. Consequently, improved heat rate performance is directly associated with reduced fuel consumption and enhanced overall operational efficiency [26]. In Steam Power Plant operation, heat rate is widely used as a key indicator of thermal efficiency, reflecting the effectiveness of converting thermal energy into electrical output. It is commonly expressed as the amount of energy required—typically in British Thermal Units (BTU)—to produce one kilowatt-hour (kWh) of electricity [27]. Therefore, the lower the heat rate value, the more efficient the power generation system becomes, since a smaller amount of fuel energy is consumed to generate the same electrical output. Mathematically, the heat rate (HR) can be calculated using the following Eq. (4) for the gross plant heat rate and use Eq. (5) for the net plant heat rate [28]:

$$\text{Gross plant heat rate (GPHR)} = \frac{B \times \text{HHV}}{\text{GGO}} \quad (4)$$

$$\text{Net plant heat rate (NPHR)} = \frac{B \times \text{HHV}}{\text{NettGO}} \quad (5)$$

Specific Fuel Consumption (SFC) is a performance parameter used to evaluate the efficiency of a combustion system in converting fuel into useful energy output. SFC is defined as the amount of fuel consumed per unit of power generated, thereby providing an indication of how effectively a machine or power plant utilizes fuel during operation. In thermal power generation systems, SFC is commonly expressed as the quantity of fuel required to produce a specific amount of electrical energy (kWh). A lower SFC value indicates superior operational efficiency, as a smaller quantity of fuel is required to generate the same electrical output. Conversely, higher SFC values reflect less efficient fuel utilization and increased operational costs. Therefore, SFC is widely employed as a key performance indicator in evaluating combustion efficiency, fuel economy, and the overall operational effectiveness of power plants, particularly under varying fuel compositions such as coal and biomass co-firing conditions. Specific Fuel Consumption (SFC) can be calculated using the following Eq. (6):

$$\text{SFC Net} = \frac{Q_f}{\text{kWh}_{\text{net}}} \quad (6)$$

2.6 Statistical Analysis

The two-way analysis of variance (ANOVA) with replication simultaneously tests the effects of varying two

variables (such as gender and age or wealth and geographic area, and their interaction) for a sample which consists of more than one respondent per a certain combination of variables. While in two-factor ANOVA without replication there was only one sample item (observation) for each combination of factors [29]. Two-Way ANOVA with replication, used to evaluate the effect of Area/location, Fuel type and Interaction effects in Corrosion Rate and Remaining Life.

Linear Regression is a statistical method used to examine the relationship between one dependent variable and two or more independent variables simultaneously [30]. This approach enables researchers to quantify the extent to which multiple predictor variables influence a response variable, while also identifying the direction and magnitude of each effect. The regression coefficients indicate the expected change in the dependent variable associated with a one-unit increase in the corresponding independent variable while holding other variables constant [31]. Positive coefficients indicate a direct relationship, whereas negative coefficients represent an inverse relationship. Linear Regression, used to analyze relationships between: Calorific value-NPHR and Calorific values-SFC.

III. RESULTS AND DISCUSSIONS

3.1 Corrosion Rate Analysis

The corrosion rate data were analyzed using a Two-Way ANOVA with replication, and the results are summarized in Table 1.

Table 1: Result of Two-way Anova Corrosion rate Unit 1 and Unit 2

Unit 1	Type III SS	df	MS	F	Sig.	η^2_p
Area	0.530	3	0.177	949.580	0.000	0.762
Fuel	1.480	1	1.480	7955.204	0.000	0.900
Area*Fuel	0.078	3	0.026	139.986	0.000	0.321
Error	0.165	888	0.000			
Unit 2	Type III SS	df	MS	F	Sig.	η^2_p
Area	0.262	3	0.087	584.417	0.000	0.664
Fuel	0.573	1	0.573	3835.156	0.000	0.812
Area*Fuel	0.039	3	0.013	86.885	0.000	0.227
Error	0.133	888	0.000			

The results indicate that all examined variables have a statistically significant effect on Corrosion rate ($p < 0.05$), confirming their relevance in explaining variations in material degradation. Among these factors, fuel type exhibits the most dominant influence, with partial eta squared (η^2_p) values of 0.900 for Unit 1 and 0.812 for Unit 2, indicating a very large

effect size and strong explanatory power. Spatial variation (area/location) also demonstrates a substantial contribution, with η^2_p values of 0.762 and 0.664, reflecting a moderate-to-high effect on corrosion rate. In contrast, the interaction between variables shows a comparatively smaller yet still meaningful effect, with η^2_p values of 0.321 for Unit 1 and

0.227 for Unit 2. These findings suggest that while combined operational factors influence corrosion rate, their contribution is less pronounced than the independent effects of fuel type and location.

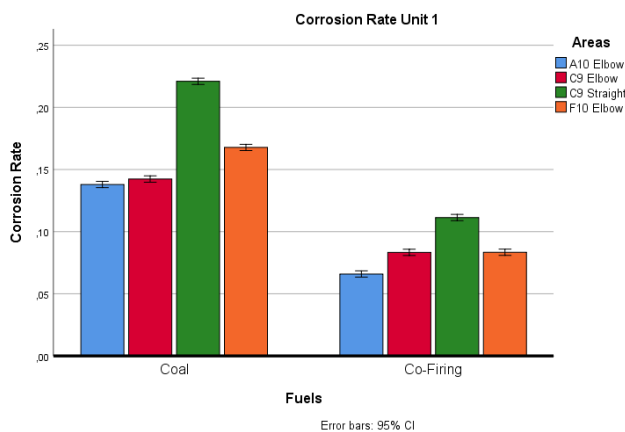


Figure 3: Corrosion Rate Chart Unit 1

The diagram in Figure 3. indicates that the corrosion rate associated with coal-fired operation is consistently higher than that observed under co-firing conditions across all monitored boiler tube locations. The average corrosion rates for coal combustion are recorded as 0.1379 mm/year at A10 Elbow, 0.1423 mm/year at C9 Elbow, 0.2210 mm/year at C9 Straight, and 0.1678 mm/year at F10 Elbow. The results highlight that the C9 Straight section exhibits the highest corrosion rate among all evaluated locations. This trend is evident under both fuel conditions, with a corrosion rate of 0.2210 mm/year for coal firing and 0.1113 mm/year for co-firing.

3.2 Remaining Life Analysis

The remaining life data analyzed using a two-way ANOVA with replication. This analytical approach enables the simultaneous evaluation of the main effects of each factor, as well as their interaction effects, thereby providing a comprehensive understanding of how different variables influence the remaining life of boiler tubes under varying operating conditions. The data are presented in Table 2.

Table 2: Result of Two-way Anova Remaining Life Unit 1 and Unit 2

Unit 1	Type III SS	df	MS	F	Sig.	η^2_p
Area	477.85	3	159.282	49.22	0.000	0.143
Fuel	31006.07	1	1006.07	9582.04	0.000	0.915
Area*Fuel	1571.74	3	523.91	161.91	0.000	0.354
Error	2873.44	888	3.24			
Unit 2	Type III SS	df	MS	F	Sig.	η^2_p
Area	228.97	3	76.32	60.99	0.000	0.171
Fuel	10076.14	1	10076.14	8052.89	0.000	0.901
Area*Fuel	419.52	3	139.84	111.76	0.000	0.274
Error	1111.11	888	1.25			

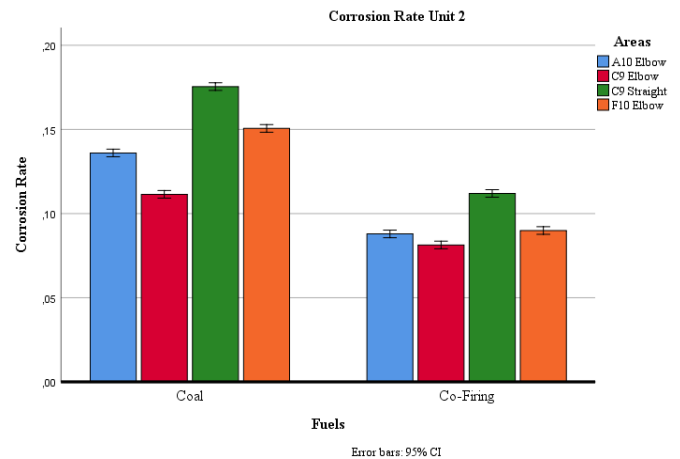


Figure 4: Corrosion Rate Chart Unit 2

The diagram in Figure 4. demonstrates that corrosion rates under coal-fired operation are consistently higher than those observed during co-firing across all evaluated boiler tube locations. The average corrosion rates for coal combustion are reported as 0.1360 mm/year at A10 Elbow, 0.1114 mm/year at C9 Elbow, 0.1754 mm/year at C9 Straight, and 0.1506 mm/year at F10 Elbow. In addition, the C9 Straight section exhibits the highest corrosion rate among all monitored areas. This pattern is consistent under both operating conditions, with corrosion rates of 0.1754 mm/year for coal firing and 0.1120 mm/year for co-firing. These results indicate that, although co-firing contributes to a reduction in overall corrosion rates [32], certain critical locations particularly C9 Straight remain more vulnerable to accelerated material degradation compared to other sections of the boiler tubing system.

All examined variables exert a statistically significant influence on the remaining life of boiler tubes ($p < 0.05$), indicating that both operational and spatial factors contribute to material degradation. Among these, fuel type emerges as the dominant factor, with partial eta squared (η^2_p) values of 0.915 for Unit 1 and 0.901 for Unit 2, reflecting a very large effect size. The interaction between variables demonstrates a moderate effect, with η^2_p values of 0.354 and 0.274 for Unit 1 and Unit 2, respectively, suggesting that combined operational conditions play a meaningful role in influencing remaining life. In contrast, the effect of spatial variation (area/location) is comparatively smaller, with η^2_p values of 0.143 and 0.171, although still statistically significant.

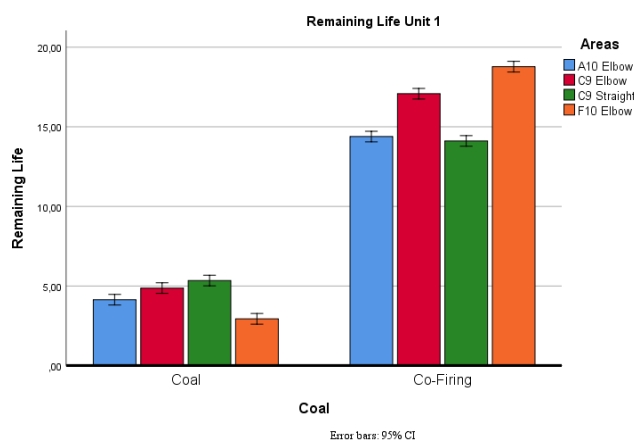


Figure 5: Remaining Life Chart Unit 1

The diagram in Figure 5. indicates that, overall, the remaining life of boiler tubes under co-firing operation is substantially longer than that observed under conventional coal combustion. The maximum remaining life under co-firing conditions is recorded at the F10 Elbow location, with a value of 18.7759 years, while the minimum occurs at the C9 Straight section, with a remaining life of 14.1106 years.

Boiler tubes operating under coal-fired conditions exhibit significantly shorter remaining life. The highest value is observed at the C9 Straight location, reaching 5.3435 years, whereas the lowest remaining life is identified at the F10 Elbow, with only 2.9390 years. These findings clearly demonstrate the beneficial impact of biomass co-firing in extending boiler tube service life, while also highlighting the presence of location-specific variability in degradation behavior.

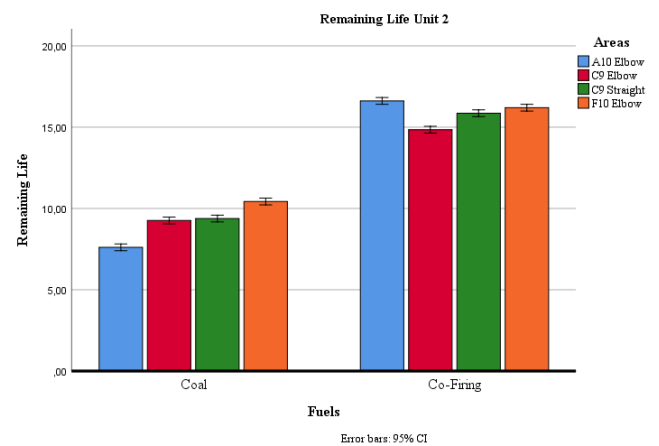


Figure 6: Remaining Life Chart Unit 2

The diagram in Figure 6. illustrates that, overall, the remaining life of boiler tubes under co-firing conditions is consistently longer than that observed with conventional coal firing. The longest remaining life under co-firing is identified at the A10 Elbow location, with a value of 16.6162 years, while the shortest is recorded at the C9 Elbow, at 14.8454 years. In contrast, boiler tubes operating with coal fuel exhibit comparatively shorter service life. The highest remaining life under coal firing is observed at the F10 Elbow, reaching 10.4309 years, whereas the lowest value is found at the A10 Elbow, with only 7.6104 years. These results further reinforce the advantage of co-firing in extending boiler tube longevity, while also indicating spatial variability in degradation patterns across different tube locations.

3.3 NPHR and Calorific Value Analysis

Results of the linear regression analysis for Nett Plant Heat Rate (NPHR) are presented in the Table 3.

Table 3: Result of Linear Regression NPHR and Calorific Value Unit 1 and Unit 2

Unit		β	Std. Error	Beta	t	Sig.
Unit 1	Constant	-303.119	713.474		-0.425	0.673
	Coal	0.699	0.159	0.523	4.382	0.000
	Co-Firing	-0.091	0.254	-0.050	-0.357	0.722
Unit 2	Constant	1625.290	586.020		2.773	0.008
	Coal	0.270	0.130	0.275	2.064	0.044
	Co-Firing	0.040	0.226	0.024	0.171	0.865

*Dependent Variable: NPHR

The regression results indicate that, in Unit 1, coal calorific value exhibits a positive coefficient ($\beta = 0.699, p < 0.05$), suggesting a significant direct relationship with Net Plant Heat Rate (NPHR). This implies that an increase in coal calorific value is associated with a corresponding rise in NPHR, indicating reduced thermal efficiency. In contrast, co-firing shows a negative coefficient ($\beta = -0.091$) with a high p-value ($p = 0.722 > 0.05$), indicating an inverse but statistically insignificant relationship with NPHR. For Unit 2, both coal and co-firing display positive coefficients ($\beta = 0.270, p = 0.044 < 0.05$ and $\beta = 0.040, p = 0.865 > 0.05$, respectively). While coal calorific value has a significant positive effect on NPHR, the influence of co-firing remains weak and statistically insignificant.

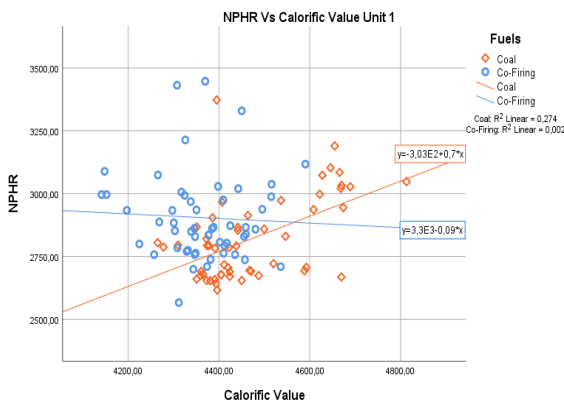


Figure 7: Comparison of NPHR and Calorific Value in Unit 1

The graph in Figure 7. further supports the previously conducted linear regression analysis. It illustrates that, under coal-fired conditions, the data exhibit a positive distribution trend, as reflected by the corresponding trendline equation $y = -3.03 \times 10^2 + 0.7 \times x$. In contrast, the co-firing condition demonstrates a negative trend, indicated by its respective trendline equation $y = 3.3 \times 10^3 - 0.09 \times x$. These opposing patterns suggest that the relationship between the analyzed variables differs substantially depending on the fuel type, reinforcing the conclusions derived from the regression model.

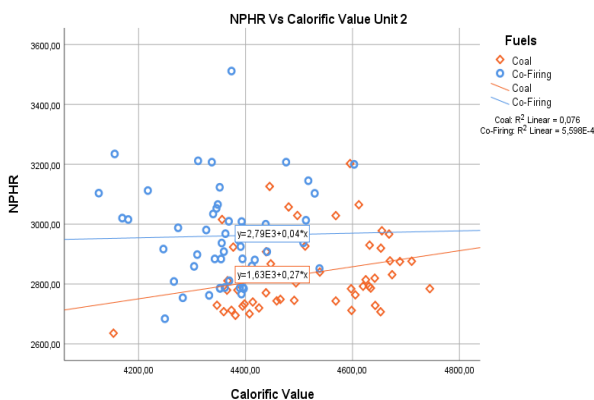


Figure 8: Comparison of NPHR and Calorific Value in Unit 2

The relationship between Net Plant Heat Rate (NPHR) and the calorific value of coal that shown in the Figure 8. exhibits a positive distribution pattern, as previously identified in the analysis presented in Table 3. This positive relationship is reflected in the corresponding trendline equation $y = 1.63 \times 10^3 + 0.27 \times x$, indicating that variations in calorific value are associated with proportional changes in NPHR.

A similar pattern is observed under co-firing conditions, where the relationship between NPHR and calorific value also demonstrates a positive trend, as indicated by its respective trendline equation $y = 2.79 \times 10^3 + 0.04 \times x$. However, the graph reveals a considerable dispersion of data points, suggesting a high degree of variability within the dataset. This indicates that calorific value alone does not fully explain the variation in NPHR.

3.4 SFC and Calorific Value Analysis

The outcomes of the linear regression analysis performed for Specific Fuel Consumption (SFC) are comprehensively presented in the following tables and graphical representations, providing a detailed evaluation of the relationship between calorific value and fuel consumption performance under varying operating conditions. The result as shown in the Table 4.

Table 4: Result of Linear Regression SFC and Calorific Value Unit 1 and Unit 2

Unit 1		β	Std. Error	Beta	t	Sig.
1	Constant	0.576	0.149		3.870	0.000
	Coal	3.298E-6	0.000	0.014	0.099	0.921
2	Constant	1.313	0.234		5.609	0.000
	Co-Firing	-1.590E-4	0.000	-0.384	-2.970	0.005
Unit 2		β	Std. Error	Beta	t	Sig.
1	Constant	0.909	0.099		9.215	0.000
	Coal	-7.123E-5	0.000	-0.412	-3.260	0.002
2	Constant	1.261	0.208		6.079	0.000
	Co-Firing	-1.440E-4	0.000	-0.388	-3.036	0.004

*Dependent Variable: SFC

The regression results in Unit 1 reveal that coal fuel exhibits a positive coefficient (3.298×10^{-6}), indicating that an increase in calorific value is associated with a marginal rise in SFC. In contrast, co-firing demonstrates a negative coefficient (-1.590×10^{-4}), indicating that higher calorific values lead to a reduction in SFC. These findings are further supported by the graphical analysis, where coal exhibits a weak positive trendline, while co-firing shows a clearer negative trend, reinforcing the inverse relationship between calorific value and SFC under co-firing conditions. The regression analysis in Unit 2 indicates that the calorific value of coal and co-firing

exhibits a negative coefficient (-7.123×10^5) and (-1.440×10^4) implying that an increase in coal calorific value leads to a reduction in SFC. Suggesting that coal and co-firing calorific value plays an important role in influencing fuel consumption efficiency [33].

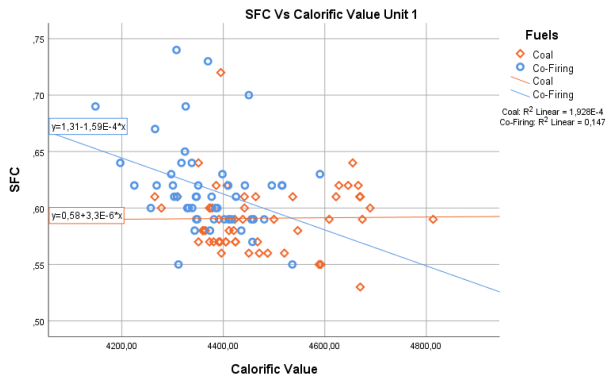


Figure 9: Comparison of SFC and Calorific Value in Unit 1

The comparative graph in Figure 9. indicates that coal-fired operation exhibits a positive distribution pattern, consistent with the results of the preceding regression analysis. This positive relationship is reflected in the coal trendline, described by the equation $y = 0.58 + 3.3 \times 10^{-6}x$, suggesting that increases in calorific value are associated with a proportional increase in SFC. In contrast, the co-firing condition demonstrates an inverse relationship, as indicated by the negative trendline equation $y = 1.31 - 1.59 \times 10^{-4}x$. This implies that higher calorific values under co-firing are associated with a reduction in SFC. Furthermore, the scatter plot reveals a substantial dispersion of data points, highlighting considerable variability within the dataset. This suggests that calorific value alone does not fully explain variations in SFC.

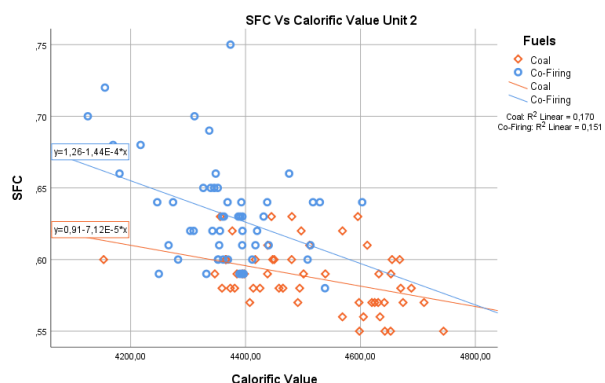


Figure 10: Comparison of SFC and Calorific Value in Unit 1

The graph in Figure 10. further substantiates the linear regression analysis presented in Tables 4. The relationship between calorific value and SFC under coal-fired conditions is represented by the trendline equation $y = 0.91 - 7.12 \times 10^{-5}x$, indicating a positive association. In contrast, the co-firing

condition exhibits a negative relationship, as reflected by the trendline equation $y = 1.26 - 1.44 \times 10^{-4}x$, suggesting that increasing calorific value is associated with a reduction in SFC. Moreover, the scatter plot demonstrates a wide dispersion of data points, indicating substantial variability within the dataset. This variability implies that calorific value alone is not the sole determinant of SFC.

IV. CONCLUSIONS

This study demonstrates that biomass co-firing significantly influences corrosion rate and remaining life of boiler tube and overall power plant performance at PLTU Banten 2 Labuan. The statistical analysis confirms that area/location, fuel type, and their interaction have a significant effect on both corrosion rate (CR) and remaining life (RL) ($p < 0.05$). Among these variables, fuel type emerges as the dominant factor, with very large effect sizes have partial eta squared (η_p^2) values 0.900 (Unit 1), 0.812 (Unit 2) in corrosion rate and 0.915 (Unit 1) and 0.901 (Unit 2) in remaining life, indicating that the choice of fuel plays a critical role in determining material degradation and remaining life behavior.

From a performance perspective, regression analysis indicates that calorific value plays a key role in determining both Net Plant Heat Rate (NPHR) and Specific Fuel Consumption (SFC). The results indicate that coal-fired operation generally exhibits a positive distribution pattern for both NPHR and SFC with coefficient 0.7, 0.27 and 3.3×10^{-6} exceptions are observed in the SFC analysis for Unit 2, where coefficient values -7.12×10^{-5} demonstrate negative distributions. Under co-firing conditions predominantly shows negative distribution trends for both NPHR and SFC, with coefficient values of -0.09, -1.59×10^{-4} , and -1.44×10^{-4} , indicating an inverse relationship between the evaluated variables, an exception is identified in the NPHR analysis for Unit 2, where coefficient 0.04 exhibits a positive distribution pattern. These findings suggest that the relationship between calorific value, fuel composition, and plant performance parameters varies depending on operational configuration and unit-specific characteristics.

REFERENCES

- [1] P. Adhiguna, "Indonesia's Biomass Cofiring Bet: Beware of the Implementation Risks," *Institute for Energy Economics and Financial Analysis (IEEFA)*, 2021, [Online] https://ieefa.org/sites/default/files/2022-06/Indonesias-Biomass-Cofiring-Bet_February-2021.pdf
- [2] PT PLN (Persero), "Rencana Usaha Penyediaan Tenaga listrik (RUPTL) 2021-2030". *Jakarta: PT PLN (Persero)*, 2021 [Online]

- <https://web.pln.co.id/statics/uploads/2021/10/ruptl-2021-2030.pdf>
- [3] M. Triani, F. Tanbar, N. Cahyo, R. Sitanggang, D. Sumiarsa & G. L. Utama, "The Potential Implementation of Biomass Co-firing with Coal in Power Plant on Emission and Economic Aspects: A Review," *Eksakta: Journal of Sciences and Data Analysis*, vol. 3, no. 2, pp. 83-94, 2022, doi: <https://doi.org/10.20885/EKSAKTA.vol3.iss2.art4>
- [4] J. P. Silva, S. Teixeira, E. Grilo, B. Peters & J. C. Teixeira, "Analysis and Monitoring of the Combustion Performance in a Biomass Power Plant," *Cleaner Engineering and Technology*, vol. 5, pp. 1-14, 2021, doi: <https://doi.org/10.1016/j.clet.2021.100334>
- [5] N. Cahyo, E. Hariyostanto & H. Hariana, "An Evaluation of Co-firing Palm Kernel Shell with Coal on CFB Power plant," *2022 International Conference on Technology and Policy in Energy and Electric Power (ICT-PEP)*, pp. 168-173, 2022, doi: <https://doi.org/DOI:10.1109/ICT-PEP57242.2022.9988937>
- [6] E. Amirabedin, M. Pooyanfar, M. A. Rahim & H. Topal, "Techno-Environmental Assessment Of Co Gasification Of Low-Grade Turkish Lignite With Biomass In A Trigeneration Power Plant," *Environmental and Climate Technologies*, vol. 13, pp. 5-11, 2014, doi: <https://doi.org/10.2478/rtuct-2014-0001>
- [7] N. Cahyo, H. H. Alif, I. A. Aditya & H. D. Saksono, "Co-firing characteristics of wood pellets on pulverized coal power plant," *IOP Conference Series: Materials Science and Engineering*, vol. 1098, pp. 1-7, 2021, doi: <https://doi.org/10.1088/1757-899X/1098/6/062088>
- [8] P. Picciano, F. X. Aguilar, D. Burtraw & A. Mirzaee, "Environmental and socio-economic implications of woody biomass co-firing at coal-fired power plants," *Resource and Energy Economics*, vol. 68, pp. 1-13, 2022, doi: <https://doi.org/10.1016/j.reseneeco.2022.101296>
- [9] M. Anshar, A. S. Kader & F. N. Ani, "The Utilization Potential Of Rice Husk As An Alternative Energy Source For Power Plants In Indonesia," *Advanced Materials Research*, vol. 845, pp. 494-498, 2022, doi: <https://doi.org/10.4028/www.scientific.net/AMR.845.494>
- [10] Y. Yunaidi, F. Surahmanto & S. Harnowo, "The Risk Analysis Of Rice Husk Of Co-Firing Fuel For Boilers In Sugar Mills," *Journal of Physics: Conference Series*, vol. 1446, pp. 1-8, 2020, doi: <https://doi.org/10.1088/1742-6596/1446/1/012041>
- [11] R. Prokeš, J. Diviš, J. Ryšavý, L. Jezerská, L. Niedzwiecki, D. P. Vilas, K. Moscicki, A. Mlonka-Medrala, W. Yan, D. Žurovec & J. Cespiva, "Thermomechanical Treatment of SRF for Enhanced Fuel Properties," *Fire*, vol. 8, no. 2, pp. 1-20, 2025, doi: <https://doi.org/10.3390/fire8020057>
- [12] B. Morrison & J. S. Golden, "Life cycle assessment of co-firing coal and wood pellets in the Southeastern United States," *Journal of Cleaner Production*, vol. 150, pp. 188-196, 2017, doi: <https://doi.org/10.1016/j.jclepro.2017.03.026>
- [13] M. Soleh, A. H. Ahmad, F. B. Juangsa, P. S. Darmanto & A. D. Pasek, "Impact of Different Kinds of Biomass Mixtures on Combustion Performance, Interaction and Synergistic Effects in Cofiring of Coal and Biomass in Steam Power Plants," *Clean Energy*, vol. 7, no. 5, pp. 1136-1147, 2023, doi: <https://doi.org/10.1093/ce/zkad049>
- [14] F. Tanbar, N. Cahyo & M. Zahoor, "Characteristics of Co-firing Solid Recovered Fuel with sub-bituminous Coal on Pulverized Coal Boiler Power Plant 300 MWe," *E3S Web of Conferences*, vol. 432, pp. 1-8, 2023, doi: <https://doi.org/10.1051/e3sconf/202343200009>
- [15] X. Wang, Z. U. Rahman, Z. Lv, Y. Zhu, R. Ruan, S. Deng, L. Zhang & H. Tan, "Experimental Study and Design of Biomass Co-Firing in a Full-Scale Coal-Fired Furnace with Storage Pulverizing System," *Agronomy*, vol. 11, no. 4, pp. 1-11, 2021, doi: <https://doi.org/10.3390/agronomy11040810>
- [16] A. Sugiyono, I. Febijanto, E. Hilmawan & A. Adiarso, "Potential of biomass and coal co-firing power plants in Indonesia: a PESTEL analysis," *IOP Conference Series: Earth and Environmental Science*, vol. 963, pp. 1-11, 2022, doi: <https://doi.org/10.1088/1755-1315/963/1/012007>
- [17] H. Hariana, P. Prabowo, E. Hilmawan, F. M. Kuswa, A. Darmawan & M. Aziz, "A comprehensive evaluation of cofiring biomass with coal and slagging-fouling tendency in pulverized coal-fired boilers," *Ain Shams Engineering Journal*, vol. 14, no. 7, pp. 1-10, 2023, doi: <https://doi.org/10.1016/j.asej.2022.102001>
- [18] E. Agbor, X. Zhang & A. Kumar, "A Review Of Biomass Co-Firing In North America," *Renewable and Sustainable Energy Reviews*, vol. 40, pp. 930-943, 2014, doi: <https://doi.org/10.1016/j.rser.2014.07.195>
- [19] W. M. Griffin, J. Michalek, H. S. Matthews & M. N. Hassan, "Availability of Biomass Residues for Cofiring in Peninsular Malaysia: Implications for Cost and GHG Emissions in the Electricity Sector," *Energies*, vol. 7, no. 2, pp. 804-823, 2014, doi: <https://doi.org/10.3390/en7020804>
- [20] C. Ndibe, J. Maier & G. Scheffknecht, "Combustion, Co-Firing And Emissions Characteristics Of Torrefied

- Biomass In A Drop Tube Reactor,” *Biomass and Bioenergy*, vol. 79, pp. 105-115, 2015, doi: <https://doi.org/10.1016/j.biombioe.2015.05.010>
- [21] B. N. Madanayake, S. Gan, C. Eastwick & H. K. Ng, “Biomass as an energy source in coal cofiring and its feasibility enhancement via pre-treatment techniques,” *Fuel Processing Technology*, vol. 159, pp. 287-305, 2017, doi: <https://doi.org/10.1016/j.fuproc.2017.01.029>
- [22] M. V. Gil & F. Rubiera, “5 - Coal And Biomass Cofiring: Fundamentals And Future Trends,” *New Trends in Coal Conversion Combustion Gasification Emissions and Coking*, pp. 117-140, 2019, doi: <https://doi.org/10.1016/B978-0-08-102201-6.00005-4>
- [23] F. Tanbar, S. Purba, A. S. Samsudin, E. Supriyanto & I. A. Aditya, “Analisa Karakteristik Pengujian Co-Firing Biomassa Sawdust Pada Pltu Type Pulverized Coal Boiler Sebagai Upaya Bauran Renewable Energy,” *Offshore Oil Production facilities and Renewable Energy*, vol. 5, no. 2, pp. 50-56, 2021, doi: <https://doi.org/10.30588/jo.v5i2.928>
- [24] American Petroleum Institute, “API 510: Pressure Vessel Inspection Code: In-Service Inspection, Rating, Repair, and Alteration,” Vol. Ninth Edition, *Washington: API Publishing Services*, 2006.
- [25] A.S. Haqim, W. A. Mohamed & A. S. Tijani, “Performance degradation analysis of a medium pressure superheater due to tube deactivation,” *Journal of Mechanical Engineering and Sciences*, vol. 17, no. 2, pp. 9443-9452, 2023, doi: <https://doi.org/10.15282/jmes.17.2.2023.3.0747>
- [26] M. A. Roni, M. Z. Abedin, S. Islam, M. A. Miah & Z. Ahsan, “Thermodynamic Analysis and Performance Improvement in Biomass Power Plant: A Comprehensive Review,” *American Journal of Mechanical and Materials Engineering*, vol. 8, no. 1, pp. 1-14, 2023, doi: <https://doi.org/10.11648/j.ajmme.20240801.11>
- [27] Y. C. Dwiaji, “Analisis Pengaruh Co-Firing Biomassa Terhadap Kinerja Peralatan Boiler,” *Journal of Applied Mechanical Engineering and Renewable Energy (Jamere)*, vol. 3, no. 1, pp. 7-15, 2023, doi: <https://doi.org/10.52158/jamere.v3i1.445>
- [28] K. Darmawan, L. C. Permadi, B. C. Tjiptady, R. F. Meditama, I. M. Fitriani & F. K. Asshidiqi, “Analysis of Heat Rate Co-firing Pacitan PLTU,” *G-Tech: Jurnal Teknologi Terapan*, vol. 9, no. 1, pp. 410-416, 2025, doi: <https://doi.org/10.70609/gtech.v9i1.6211>
- [29] S. Białowas, “Experimental Design and Biometric Research Toward Innovations,” *Poznan: PUEB Press*, 2021, doi: <https://doi.org/10.18559/978-83-8211-079-1>
- A. R. Kamel & M. R. Abonazel, “A Simple Introduction to Regression Modeling using R,” *Computational Journal of Mathematical and Statistical Sciences*, vol. 2, no. 1, pp. 52-79, 2023, doi: <https://doi.org/10.21608/cjms.2023.189834.1002>
- [30] N. Roustaei, “Application and Interpretation of Linear-regression Analysis,” *Medical Hypothesis Discovery and Innovation in Ophthalmology*, vol. 13, no. 3, pp. 151-159, 2024, doi: <https://doi.org/10.51329/mehdiophthal1506>
- [31] Y. Wang, Y. Sun, L. Jiang, L. Liu & Y. Li, “Characteristics of Corrosion Related to Ash Deposition on Boiler Heating Surface during Cofiring of Coal and Biomass,” *Journal of Chemistry*, vol. 2020, pp. 1-9, 2020, doi: <https://doi.org/10.1155/2020/1692598>
- [32] Z. Nawaz & U. Ali, “Techno-economic Evaluation of Different Operating Scenarios for Indigenous and Imported Coal Blends and Biomass Co-firing on Supercritical Coal Fired Power Plant Performance,” *Energy*, vol. 212, pp. 1-13, 2020, doi: <https://doi.org/10.1016/j.energy.2020.118721>

Citation of this Article:

Rifqi Jauhari, Hadiyanto, & Sri Widodo Agung Suedy. (2026). Analysis of Biomass Co-Firing Impact on Boiler Tube Corrosion Rate in Steam Power Plants. *International Research Journal of Innovations in Engineering and Technology - IRJIET*, 10(5), 673-682. Article DOI <https://doi.org/10.47001/IRJIET/2026.105090>
